

AD-787 436

AN EXPERIMENTAL INVESTIGATION OF  
SHORT DIFFUSERS FOR GAS DYNAMIC LASERS

John Joseph Zerr

Naval Postgraduate School  
Monterey, California

June 1974

This Document  
Reproduced From  
Best Available Copy

DISTRIBUTED BY:



National Technical Information Service  
U. S. DEPARTMENT OF COMMERCE  
5285 Port Royal Road, Springfield Va. 22151

## **REPRODUCTION QUALITY NOTICE**

**This document is the best quality available. The copy furnished to DTIC contained pages that may have the following quality problems:**

- **Pages smaller or larger than normal.**
- **Pages with background color or light colored printing.**
- **Pages with small type or poor printing; and or**
- **Pages with continuous tone material or color photographs.**

**Due to various output media available these conditions may or may not cause poor legibility in the microfiche or hardcopy output you receive.**



**If this block is checked, the copy furnished to DTIC contained pages with color printing, that when reproduced in Black and White, may change detail of the original copy.**

AD787436

REPORT DOCUMENTATION PAGE		READ INSTRUCTIONS BEFORE COMPLETING FORM
1. REPORT NUMBER	2. GOVT ACCESSION NO.	3. RECIPIENT'S CATALOG NUMBER
4. TITLE (and Subtitle)  An Experimental Investigation of Short Diffusers for Gas Dynamic Lasers		5. TYPE OF REPORT & PERIOD COVERED  Master's Thesis June 1974
7. AUTHOR(s)  John Joseph Zerr		6. PERFORMING ORG. REPORT NUMBER
9. PERFORMING ORGANIZATION NAME AND ADDRESS  Naval Postgraduate School Monterey, California 93940		10. PROGRAM ELEMENT, PROJECT, TASK AREA & WORK UNIT NUMBERS
11. CONTROLLING OFFICE NAME AND ADDRESS  Naval Postgraduate School Monterey, California 93940		12. REPORT DATE June 1974
14. MONITORING AGENCY NAME & ADDRESS (if different from Controlling Office)		13. NUMBER OF PAGES 52
		15. SECURITY CLASS. (of this report)  Unclassified
		16. DECLASSIFICATION/DOWNGRADING SCHEDULE
16. DISTRIBUTION STATEMENT (of this Report)  Approved for public release; distribution unlimited.		
17. DISTRIBUTION STATEMENT (of the abstract entered in Block 20, if different from Report)		
18. SUPPLEMENTARY NOTES  Reproduced by NATIONAL TECHNICAL INFORMATION SERVICE U S Department of Commerce Springfield VA 22151		
19. KEY WORDS (Continue on reverse side if necessary and identify by block number)		
20. ABSTRACT (Continue on reverse side if necessary and identify by block number)  One of the largest components of a gas dynamic laser is the diffuser. A significant reduction in the size of this component could represent a significant savings in the size and weight of the entire system. The purpose of this investigation was to examine several short supersonic diffuser designs with fixed walls and no boundary layer control. Thick diffusers with shallow ramp angles are supposed to provide optimum pressure recovery for fixed diffusers. It was found in this investigation, however, that no loss of pressure		

recovery is suffered when steep ramp angles and thin diffusers are used. Steep ramps and thin diffuser sections would serve to minimize both the length and weight of supersonic diffusers. Start-up times were also investigated. Start-up time was found to be independent of diffuser geometry. Measured times to start were much slower than had been expected. Work beyond this thesis will seek to determine the reasons for this disparity.

An Experimental Investigation  
of Short Diffusers for Gas Dynamic Lasers

by

John Joseph Zerr  
Lieutenant Commander, United States Navy  
B.S., Purdue University, 1965

Submitted in partial fulfillment of the  
requirements for the degree of

MASTER OF SCIENCE IN AERONAUTICAL ENGINEERING

from the

NAVAL POSTGRADUATE SCHOOL  
June 1974

Author:

John J. Zerr

Approved by:

Oscar Bublary  
Thesis Advisor

Louis V. Schmid & R. W. Bell  
Chairman, Department of Aeronautics

Jack R. Borsley  
Academic Dean

## ABSTRACT

One of the largest components of a gas dynamic laser is the diffuser. A significant reduction in the size of this component could represent a significant savings in the size and weight of the entire system. The purpose of this investigation was to examine several short supersonic diffuser designs with fixed walls and no boundary layer control. Thick diffusers with shallow ramp angles are supposed to provide optimum pressure recovery for fixed diffusers. It was found in this investigation, however, that no loss of pressure recovery is suffered when steep ramp angles and thin diffusers are used. Steep ramps and thin diffuser sections would serve to minimize both the length and weight of supersonic diffusers. Start-up times were also investigated. Start-up time was found to be independent of diffuser geometry. Measured times to start were much slower than had been expected. Work beyond this thesis will seek to determine the reasons for this disparity.

## TABLE OF CONTENTS

I. INTRODUCTION-----	9
II. STATE OF KNOWLEDGE OF SUPERSONIC DIFFUSERS	10
III. EXPERIMENTAL PROGRAM-----	12
A. GENERAL-----	12
B. TEST APPARATUS-----	12
C. INSTRUMENTATION-----	14
IV. EXPERIMENTAL RESULTS-----	15
A. STARTING PRESSURE DETERMINATION-----	15
1. General Experimental Conditions-----	15
2. Starting Pressure and Diffuser Geometry -----	16
3. Diffuser Performance as a Function of Ramp Angle	18
4. Diffuser Performance as a Function of L2-----	18
5. Diffuser Performance as a Function of L1-----	19
B. FLOW VISUALIZATION-----	19
C. PRESSURE-TIME HISTORIES-----	21
V. SUMMARY AND CONCLUSIONS-----	23
DRAWINGS AND PHOTOGRAPHS-----	24
LIST OF REFERENCES-----	50
INITIAL DISTRIBUTION LIST -----	52

## LIST OF FIGURES

1. Drawing of a typical GDL.
2. Photograph of the test apparatus.
3. Diagram of the test section.
4. Photograph of the test section.
5. Diagram of the nozzle vanes.
6. Diagram of the NPS blow down wind tunnel.
7. Diagram of the Schlieren system.
8. 100 psig pressure-time trace.
9. 200 psig pressure-time trace.
10. Graph of starting pressures.
11. Legend for graphs of starting pressures.
12. Graph of starting pressures, Mach 3, 5 deg. ramp.
13. Graph of starting pressures, Mach 3, 10 deg. ramp.
14. Graph of starting pressures, Mach 3, 12 deg. ramp.
15. Graph of starting pressures, Mach 3, 15 deg. ramp.
16. Graph of starting pressures, Mach 4, 10 deg. ramp.
17. Graph of starting pressures, Mach 4, 15 deg. ramp.
18. Graph of starting pressures, Mach 4, 19 deg. ramp.
19. Theoretical plot of  $P_t/P_a$  vs.  $\Theta$ .
20. Plot of experimental  $P_t/P_a$  vs.  $\Theta$ , Mach 3.
21. Plot of experimental  $P_t/P_a$  vs.  $\Theta$ , Mach 4.
22. Plot of  $\Theta$  vs.  $L_2$ , Mach 4.
23. Photograph of separated Mach 3 flow.
24. Photograph of Mach 3 flow with center plate.

25. Photograph of non-symmetric diffuser, Mach 3.
26. Photograph of one sided diffuser, Mach 3.
27. Photograph of wave patterns, no diffuser, Mach 3.
28. Photograph of fully attached flow, Mach 3.
29. Photograph of flow separated from one wall, Mach 3.
30. Photograph of flow separated from both walls, Mach 3.
31. Photograph of Mach 4 flow, 10 deg. ramp.
32. Photograph of Mach 4 flow, 15 deg. ramp.
33. Photograph of Mach 4 flow, 19 deg. ramp.
34. Pressure-time trace for Mach 3.
35. Pressure-time trace for Mach 4.
36. Pressure-time trace for Mach 4.

## ABBREVIATIONS

<b>ft</b>	feet
<b>GDL</b>	Gas Dynamic Laser
<b>lbm</b>	pound-mass
<b>L1</b>	a characteristic length of a diffuser defined in Figure 3
<b>L2</b>	defined in Figure 3
<b>M</b>	Mach Number
<b>psia</b>	pounds per square inch absolute
<b>psig</b>	pounds per square inch gauge
<b>P<sub>a</sub></b>	atmospheric pressure, sea level
<b>P<sub>t</sub></b>	total pressure
<b>R</b>	Reynolds number
<b>Θ</b>	ramp angle

## 1. INTRODUCTION

A considerable amount of experimental work aimed at reducing total pressure losses in supersonic diffusers has been reported in the literature. Most of that work pertains to supersonic wind tunnels and jet engine inlets.<sup>1-3</sup> Intense recent interest in gas dynamic and chemical lasers has spurred extensive new research into supersonic diffuser performance.<sup>4, 5</sup>

Gas dynamic lasers (GDL) operate at Mach number of 4 to 5.5 in the laser cavity. Figure 1 shows a schematic of a typical GDL. As evident in the figure, the diffuser represents a considerable proportion of the system volume and weight. An efficient diffuser of significantly smaller dimensions is a goal of obvious merit.

For many applications, establishing supersonic flow rapidly in the GDL cavity will be important, and some GDL operations consist of a series of short bursts. Therefore, start up time is also a significant parameter.

Design criteria for supersonic diffusers for laser applications should not be as restrictive as those for wind tunnels and inlets where smooth parallel diffuser exit flow may be a necessity. For an open cycle system, there would be no such requirement on exit flow conditions. However, in a closed cycle or a multi-staged system, the nature of the exit flow again assumes importance.

## II. STATE OF KNOWLEDGE OF SUPERSONIC DIFFUSERS

Since GDL gain depends inversely on total pressure<sup>6</sup>, the role of the diffuser is to reduce the total pressure requirements and to enhance system gain.

According to Shapiro<sup>7</sup>, one of the most efficient, fixed geometry, supersonic diffusers consists of a ramp, where the area is reduced linearly, followed by a constant area section of sufficient length to allow the flow to stabilize at a subsonic Mach number, after which a subsonic expansion section can be added. Shapiro further states that without a length of constant cross sectional area after the ramp, regions of locally supersonic flow of even higher Mach number than that entering the diffuser are possible.

Experimental results<sup>8</sup> on rectangular supersonic flow channels indicate that if diffusion is accomplished through physical contraction of only one dimension of the channel, more efficiency is obtained when the larger dimension is contracted.

Reference 9 shows that pressure recovery is strongly dependent on area contraction. Pressure recovery improves as contraction ratio--the ratio of diffuser throat area to the area at the diffuser entry plane--is decreased until a certain point is reached. This point generally varies with experimental conditions, but if no boundary layer control is employed, the point occurs in the neighborhood of the theoretical limit for area contraction from the one dimensional flow model. This is about 0.6<sup>7</sup> for Mach 4.

Ramp angles for supersonic diffusers, typically, are shallow. Steep ramps produce strong oblique shocks, and as shock strength increases, separation of the boundary layer becomes more likely. Shallow ramps coupled with the requirement of significant area contraction to achieve efficient diffusion necessitate a long ramp.

Diffuser boundary layer separation generally involves two types of phenomena: 1) shock induced separation, and 2) separation due to other causes such as a radically divergent flow channel. Shock induced separation can be further subdivided into separation behind the shock generated by the leading edge of the diffuser, and separation induced by a shock incident on a diffuser surface. The first type of shock induced separation occurs when the ramp angle is large.<sup>10</sup> In this case, the separation point can occur substantially upstream of the corner. For small turning angles, only thickening of the boundary layer will occur. The second type of shock associated separation is governed principally by the Reynolds number of the boundary layer and the Mach number of the external stream.<sup>11</sup>

In essence, total pressure losses in diffusers are due to shocks and boundary layers. Losses can be somewhat limited by careful design to reduce the presence of shocks and by boundary layer removal.

One way to reduce the overall diffuser length is to use a block of wedge shaped diffuser vanes. Reference 8 reported preliminary results of experiments with this diffuser scheme.

The concept of variable geometry diffusers has been utilized for both wind tunnel and jet engine inlet designs. The maximum area contraction limit on fixed diffusers results from the necessity to

pass the starting shock through the diffuser throat. Once the supersonic flow is established, further area contraction is possible. Supersonic flow can then be maintained at a lower total pressure than that required to start the flow. The additional contraction can be accomplished either with a system of moveable diffuser walls<sup>12</sup> or aerodynamically.<sup>13</sup>

### III. EXPERIMENTAL PROGRAM

#### A. GENERAL

In 1973, a program was initiated at NPS under the auspices of Professors A. E. Fuhs and O. Biblarz to investigate GDL diffuser performance with a view toward minimizing diffuser dimensions and start up times. A computer analysis of the problem was also begun.<sup>14, 15</sup> This paper reports the results of the experimental investigation.

The experiments were concerned with two separate areas of endeavor: 1) a study of total pressures required to start supersonic flow for various diffuser geometries, and 2) determination of transients involved in the starting process.

#### B. TEST APPARATUS

Figure 2 shows the test apparatus. The apparatus consists of a supersonic wind tunnel with a bank of nozzle vanes, instead of a single supersonic nozzle, to simulate flow conditions in a GDL. The flow channel was 4 inches by 1 inch in cross section and 8.5 inches long. The one inch walls of the channel are constructed to hold a variety of diffuser pieces. The pieces were made of machined aluminum and

bolted into place. Machine tolerances were generally limited to within a few thousandths of an inch. The section of flow channel between the nozzle tips and the diffuser corresponds to a GDL cavity. Diffusion was limited to one dimension--there was no physical contraction of the 1 inch dimension. Plexiglass windows extend from the nozzle tips to the flow exit plane. The apparatus exhausts to the atmosphere and no boundary layer control is employed.

Figures 3 and 4 show the test section configured for Mach 4 operation. The average throat area is 0.126 square inches. Figure 5 shows a detail of the nozzle vanes. For Mach 3 operation there were six flow passages through the nozzle bank with an average throat area of 0.173 square inches. The measured cavity dimensions are 1.000 inch by 4.008 inches.

The NPS Department of Aeronautics blow-down wind-tunnel facility served as the flow source. The facility provides dry air which can be regulated from 0 to 250 psig. Due to this pressure limitation, the investigation was confined to Mach numbers 3 and 4.

Figure 6 shows a schematic of the blow down tunnel. In the transition section, the flow cross section is transformed from circular, with a 4 inch radius, to rectangular, 4 inches by 1 inch. The transition is accomplished through an epoxy mold inside the 12 inch long pipe of the section.

Source air temperature was measured at point B of Figure 6 with a thermocouple. The temperature in the pipe was found to decrease at 3 to 5 degrees per minute of run time. During all data runs, source air temperature variations were limited to between 40 and 80 degrees Fahrenheit.

Typical mass flows were calculated to be 2.87 lbm/sec. for Mach 3 and 2.70 lbm/sec. for Mach 4. Flow velocities in the pipe preceding the transition section were calculated to be 22.2 ft./sec. for Mach 3 and 9.1 ft./sec. for Mach 4. The velocity contribution to the total pressure was negligible.

The test condition Reynolds numbers were  $1.41 \times 10^6$  and  $1.64 \times 10^6$  at Mach numbers 3 and 4 respectively based on hydraulic diameter.

Actual Mach numbers measured from Schlieren photographs were 2.96 to 2.98 and 3.99 to 4.03.

### C. INSTRUMENTATION

The pressure at point B, Figure 6, was measured on a dial gauge with a scale of 0 to 300 psig in 5 psig increments. Cavity pressure was measured on a dial gauge with 0.5 psig increments tapped into point A. To record the pressure-time histories of a fast start, the outputs from transducers at points A and B were used alternately as the vertical inputs to a Tektronix 549 storage-type oscilloscope utilizing either a 1A6 or a 1A7 plug-in unit. The transducer at point B was a bourdon tube type, 0 to 650 psig scale and 10,000 HZ frequency response. The point A transducer was the same type except the scale was 0 to 25 psig. A piezoelectric blast transducer at point C provided the oscilloscope triggering.

Flow visualization was accomplished with a Schlieren system. Figure 7 shows the setup.

Two different start modes were used during the experiments. For determination of starting total pressures, a slow start mode was employed, whereas the pressure-time histories required a fast

start. In the slow mode, the pressure was increased gradually in 5 psig increments until a start was observed with the Schlieren. During fast starts, the pressure at point B rose from 0 psig to any preset value on the regulator valve in 0.1 seconds. Figures 8 and 9 show the pressure at point B rising to 100 psig and to 200 psig, respectively, both in the same time, 0.1 seconds.

#### IV. EXPERIMENTAL RESULTS

##### **A. STARTING PRESSURE DETERMINATION**

###### **1. General Experimental Conditions**

During the testing, length L1 (Figure 3) was varied by moving the diffuser pieces toward or away from the nozzle tips. The test section cavity length then varied as a consequence. Also, as L1 was varied, different lengths of the diffuser pieces protruded from the end of the test section. L1 only refers to the length of diffuser from the end of the ramp to the end of the plexiglass windows.

To determine the effects of cavity length variation, three tests were conducted. With the test section configuration as shown in Figure 4, an extra set of plexiglass windows was clamped onto the protruding pieces. In this way, test conditions with identical lengths, L1, but different cavity lengths could be compared. The extra windows were sealed against leaks and starting pressures were redetermined for a 15 degree ramp at Mach 3 and for 10 and 15 degree ramps at Mach 4. Dimension L2 was 0.45 inches for all three tests. For these conditions, variations of cavity length appeared to have no effect on starting pressure.

One pressure-time history was recorded for the configuration with the added windows. This was at Mach 4 with a 15 degree ramp, and again, there was no discernible effect on start up time.

To determine the effect of the protuding sections, 15 degree ramps were subjected to another set of test conditions at both Mach numbers. In this test, the pieces were sawed off so there was no protusion.  $L_1$  was varied in this manner to correspond to the data points previously obtained. Data points obtained with the sawed off pieces agreed exactly with those where protruding sections were allowed.

The actual starting pressure was, in most instances, not a sharply defined point. Variations in the starting point between runs of up to 3 psig were noted in the early stages of the experiment. For many of the conditions tested, the neighborhood of the starting point is characterized by oscillatory flow or by separated flow in the cavity. Errors in judgement as to exactly when these undesirable flow conditions had been eliminated may account for some of the scatter. Considering these conditions, it is felt that starting pressures determined are within an accuracy of  $\pm 5$  psig.

## 2. Starting Pressure and Diffuser Geometry

Preliminary tests indicated that the geometry suggested by Ref. 1 is indeed optimum. Figure 10 shows the results of tests with a particular set of wedges. Other geometries tested are discussed in section IV-B.

The major effort in this phase of the investigation was the testing of the geometry shown in Figure 11. Lengths  $L_1$ ,  $L_2$ , and  $\Theta$  were systematically varied and the starting pressures were measured.

As has been noted by other experimenters in this field, start is a meaningless term unless it is carefully defined. For some diffuser configurations, with total pressure near the starting point, flow at the desired Mach number was apparently established in some parts of the cavity but not in others. Some other undesirable flow conditions observed were separated flow in the cavity and unsteady flow. Consequently, the start can be defined, for these experiments, as steady flow established at the desired Mach number throughout the cavity with no boundary layer separation ahead of the ramp.

Results of this phase of the study are plotted in Figures 12 through 18. As can be seen from these graphs, diffuser performance involves a complicated interplay of three parameters  $L_1$ ,  $L_2$ , and  $\Theta$ .

Reference 9 reports achieving Mach 4 flow in a blow-down wind tunnel with a very long diffuser at very nearly theoretical normal-shock pressure recovery--isentropic flow exhausting through a normal shock to sea level atmospheric pressure. Adopting normal shock recovery as a performance standard, referring to Figures 12 through 16, and choosing  $P_t/P_a$  of 4.4 for Mach 3 and  $P_t/P_a$  of 10.5 for Mach 4 as reasonably attainable values, the minimum diffuser length can be determined through a simple set of calculations. The chosen  $P_t/P_a$  ratios correspond to 1.21 and 1.24 times the normal shock recovery values at Mach numbers 3 and 4 respectively.

At Mach 3, a  $P_t/P_a$  of 4.4 was achieved with a minimum overall diffuser length of 4.6 inches;  $\Theta$  was 15 degrees,  $L_1$  3.0 inches, and  $L_2$  0.45 inches. At Mach 4, a  $P_t/P_a$  of 10.5 was achieved with a minimum overall diffuser length of 5.65 inches.  $\Theta$  was 19 degrees,  $L_1$  4.5 inches, and  $L_2$  0.40 inches.

### 3. Diffuser Performance As a Function of Ramp Angle

Using a diffuser flow model wherein two oblique shocks are generated by the ramps, and a normal shock follows equilibrating the flow to atmospheric pressure,  $P_t/P_a$  was calculated for various  $\Theta$ . The results are plotted as Figure 19. Noteworthy is the fact that both the Mach 3 and Mach 4 curves have a minimum point. The experimental results are plotted vs.  $\Theta$  in Figures 20 and 21. The experimental plots were strongly influenced by parameter  $L_1$ , however there were similarities between the theoretical and experimental plots. First of all, the Mach 3 curves, both theoretical and experimental, are fairly flat. The optimum pressure recovery for both plots correspond roughly to the same general range of  $\Theta$ . The Mach 4 theoretical plot has a much more sharply defined minimum point. The Mach 4 experimental plot shows a dramatic dependence on parameter  $L_1$ . However, when  $\Theta$  vs.  $L_2$  is plotted (Figure 22) for optimum  $P_t/P_a$ , it is noted that optimum performance shifts from being a function of  $L_2$  for short  $L_1$ , to depending solely on ramp angle for longer  $L_1$ . The Mach 4 plot for  $L_1$  of 4.5 inches agrees quite well with the general features of the theoretical plot. The minimum on the experimental curve occurs at about 19 degrees and at about 22 degrees on the theoretical plot.

### 4. Diffuser Performance As a Function of $L_2$

The computer analysis (Ref. 14) indicated that for a given total pressure, diffuser performance depended on  $\Theta$  and  $L_2$  which were inversely related. That is, if  $L_2$  was large,  $\Theta$  had to be small, and vice versa. This same general tendency was evident in the experimental results.

One apparent function of parameter  $L_2$  is that, after the flow is compressed by the ramps, the thickness of the straight section prevents the incursion of adverse pressure gradients into the cavity. The adverse pressure gradient could cause separation in the cavity. It was evident from the experimental results, that a certain minimum  $L_2$  was required to prevent the adverse pressure incursion. For this set of experimental conditions, the minimum  $L_2$  which was capable of providing this adverse pressure blocking function is 0.40 inches. Each test condition involving an  $L_2$  of .35 inches was characterized by separated flow in the cavity. This region of separated flow could be forced out of the cavity by increasing total pressure. Separation of identical appearance was caused during one run where a set of wedges were installed with a 1/16 inch gap between the wedges and the channel walls. This apparently allowed adverse pressure into the cavity through the boundary layer. See Figure 23.

##### 5. Diffuser Performance As a Function of $L_1$ .

Performance was not sharply dependent on  $L_1$  at Mach 3 except at the 15 degree ramp angle. However,  $L_1$  was a very significant parameter in the Mach 4 tests.

There was a general tendency that as the ramp angle increased, the slope of the  $P_t/P_a$  vs.  $L_1$  curve increased. Also, as ramp angle increased, a greater minimum length of straight section was needed to obtain a start.

#### **B. FLOW VISUALIZATION**

Preliminary investigations sought to determine the actual flow mechanisms involved in the diffusion process. A flat plate, 1/16

inch thick, was inserted between a pair of wedge diffusers in the Mach 3 set up (see Figure 24). When the shocks from the leading edge of the diffusers were prevented from interacting, the starting value of  $P_t$  was increased.

Next, various one-sided and two-sided non-symmetrical wedge arrangements were tested. During these tests, flow separation was generally observed and performance was generally inferior to that obtained with symmetric compression schemes (see Figures 25 and 26).

Figure 27 shows the wave patterns developed with no diffuser installed in the Mach 3 set up. For this configuration, start occurred at a  $P_t/P_a$  of 9.1. Moore (Ref. 9) reports obtaining a start at Mach 3 with no diffuser at a  $P_t/P_a$  of 9.3.

During the Mach 3 tests with ramps followed by straight sections, a stall phenomenon was observed which appeared to be a function of total pressure. For diffusers which could be started at 55 psig and below, flow through the diffuser appeared to be attached to both diffuser walls (see Figure 28). If the total pressure were increased to 60 to 65 psig, the flow would separate from one diffuser wall (see Figure 29). At 85 psig, the flow would separate from both walls (see Figure 30). This corresponds roughly with the geometry related stalls discussed in Ref. 16 for subsonic diffusers.

Figures 31 through 33 are Schlieren photographs of Mach 4 tests at ramp angles of 10, 15, and 19 degrees respectively.

One incident noted in both the Mach 3 and Mach 4 tests was an apparent washing out of the diffuser leading edge shocks in the center of the channel (see Figures 28 and 32). A possible explanation is

that the boundary layer along the plexiglass surfaces may have thickened due to interaction with the ramp shock, and merely obscured the wave pattern in the flow. If this is indeed the case, the thickened boundary layer could be accomplishing a flow contraction in the one inch dimension. This gas dynamic diffusion could account, in part, for how efficient diffusion was obtained with the relatively thin diffusers and steep ramp angles.

In this investigation, separation of flow in the cavity was apparently a function of diffuser thickness ( $L_2$ ) and not of ramp angle. A small number of data points were obtained at high ramp angles, up to 20 degrees at Mach 3 and up to 30 degrees at Mach 4, and flow separation in the cavity was observed only when  $L_2$  was reduced to less than 0.40 inches.

### C. PRESSURE-TIME HISTORIES

Cavity pressure-time histories were recorded for most of the diffuser geometries tested and for both Mach numbers. However, no correlation of start times with any diffuser parameter or with total pressure variations is possible at present. Rather, start times appeared to vary randomly between 60 and 100 milliseconds. Start time here refers to the time elapsed between oscilloscope triggering and cavity pressure stabilizing at the level measured during the starting pressure tests.

The distance between points B and C of Figure 6 was 8.0 inches. The blast transducer, installed at point C, had a sensitivity of 0.15 volts/psi and the trigger threshold was 0.25 volts. The oscilloscope's trigger circuit incorporated a 200 nanosecond delay. The trace at

point B was displayed nearly in its entirety, so the wave generated by the fast start up must have been travelling at about 3300 feet per second. Calculations for a shock tube, with a pressure differential of 100 psia to 15 psia, indicated that the wave would travel at 2660 feet per second. The difference may be due to some reinforcement of the fast start up wave as it turned the right angle in the pipe after the pressure regulator valve.

Thus the initial wave must have reached the nozzle block in less than a millisecond. The reason for the relatively long start time is not apparent now, but it is hoped that high speed motion picture photography will provide the answer to this question. Equipment is being procured to accomplish this in a later stage of the NPS short diffuser program.

Occasionally, the Mach 3 set up started with a cavity pressure oscillation (see Figure 34). The occurrence of this phenomenon appeared to be random, however, when it happened, it did appear to delay start up by a few milliseconds.

Each pressure-time trace recorded for the Mach 4 tests was characterized by an undershoot, that is the cavity pressure appeared to undershoot the steady, started value (see Figures 35 and 36).

During an experimental run, the test set up did vibrate noticeably. In addition a bourdon tube transducer, mounted as shown in Figure 4, was used to obtain cavity pressure-time traces. These considerations must be further investigated before the long start up time, the pressure oscillation, and the pressure undershoot can be ascribed to gas dynamic effects.

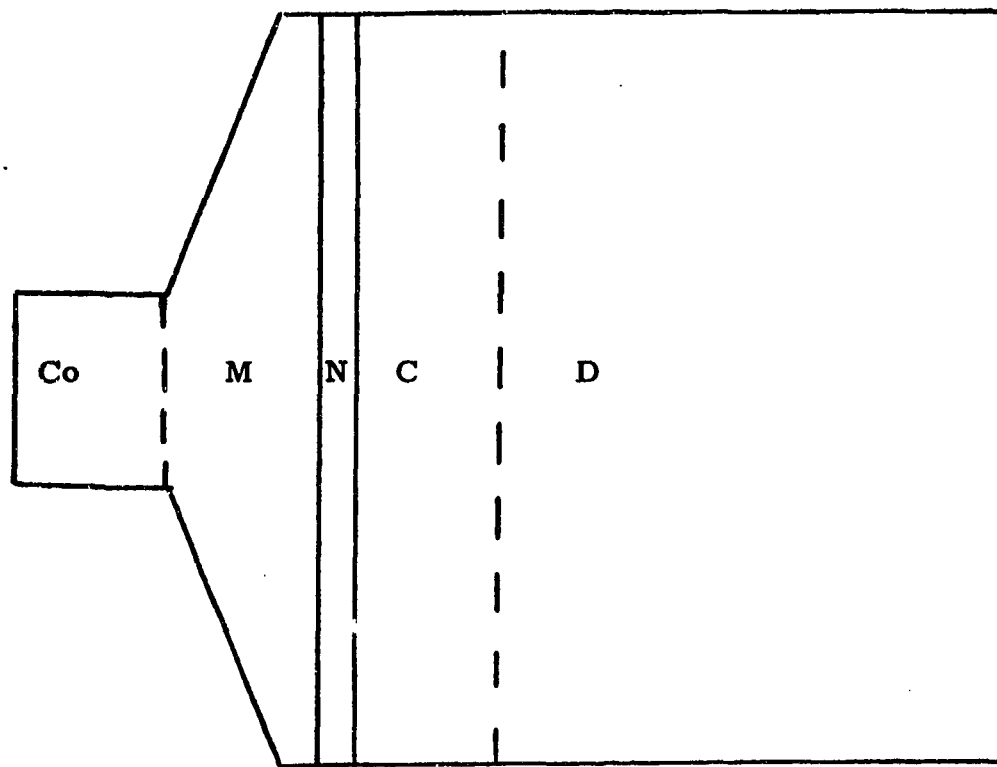
## V. SUMMARY AND CONCLUSIONS

Current supersonic diffusers generally have shallow ramp angles and thick cross sections. This study indicates, however, that the efficiency of thick diffusers with shallow ramps can be equalled and even improved upon by using steeper ramps and thin diffusers in a GDL configuration. Thus shorter diffusers seem to be a realizeable goal.

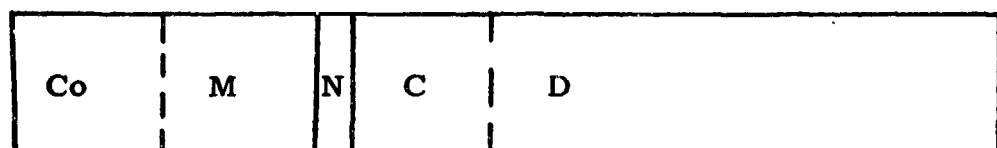
The results of this investigation indicate that diffuser performance is a complicated function of the parameters  $L_1$ ,  $L_2$ , and  $\Theta$ . Pressure recovery was not dramatically dependent on  $L_1$  at Mach 3. At Mach 4, however, there was strong dependence on  $L_1$ . At both Mach numbers tested, there was a general tendency that for shorter lengths of  $L_1$ , optimum pressure recovery was in the direction of shallow ramp angles and large  $L_2$ . For longer  $L_1$ , best pressure recovery was realized with steeper ramp angles and small  $L_2$ .

Comparing plots of  $P_t/P_a$  vs.  $\Theta$  for experimental and theoretical values, some relevant similarities were noted. At Mach 3, the two plots were similarly flat. At Mach 4, the minima of the two plots occurred at nearly the same  $\Theta$ .

Start up time appeared to be independent of diffuser variables. Measured start up times were considerably longer than had been anticipated. The start up problem is being further investigated in the continuing NPS short diffuser program.



a) Top View



b) Side View

Co = Combustor, M = Manifold, N = Nozzle block, C = Cavity  
D = Diffuser

Figure 1. Typical GDL.

BEST AVAILABLE COPY

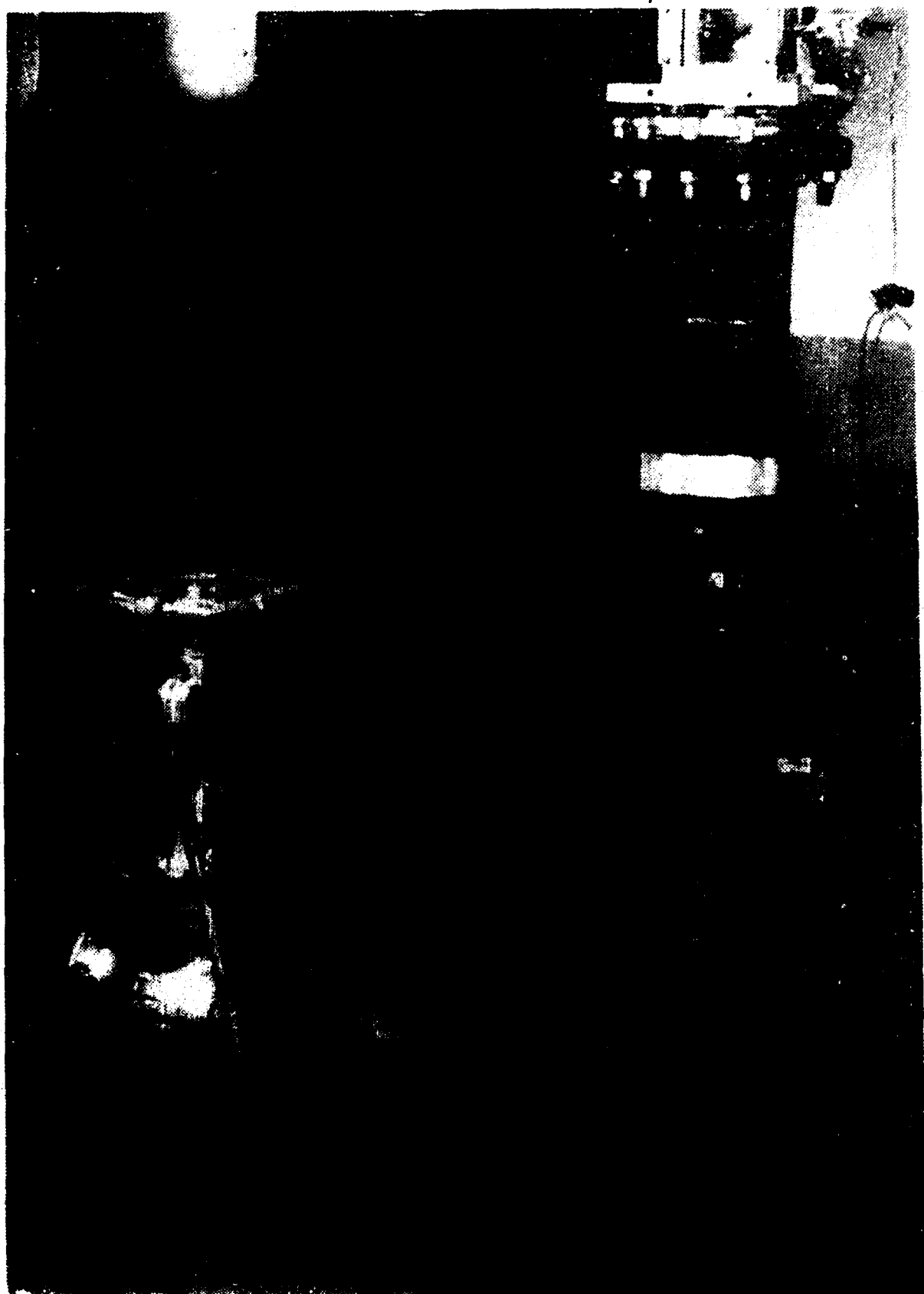


Figure 2. The NPS blow down wind tunnel.

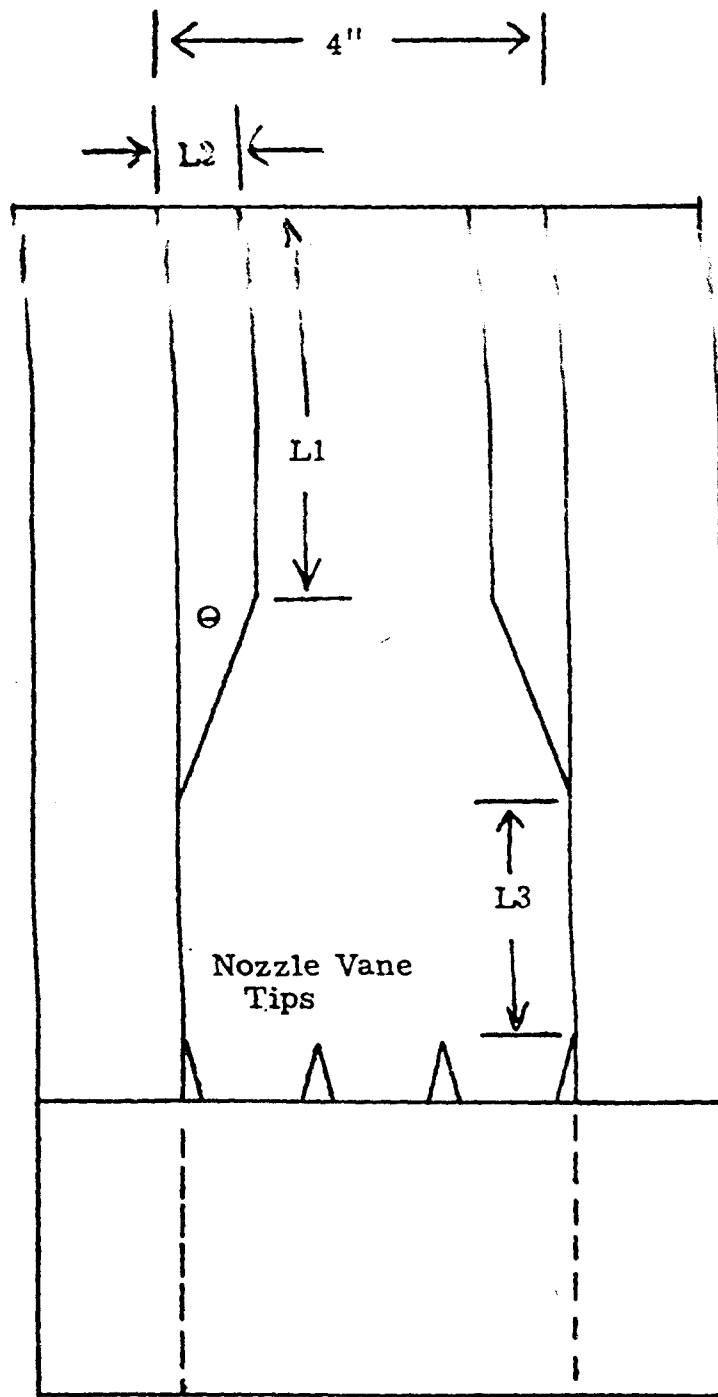


Figure 3. Test Section and Variable Diffuser Parameters.  
L3 is the Cavity Length.

BEST AVAILABLE COPY

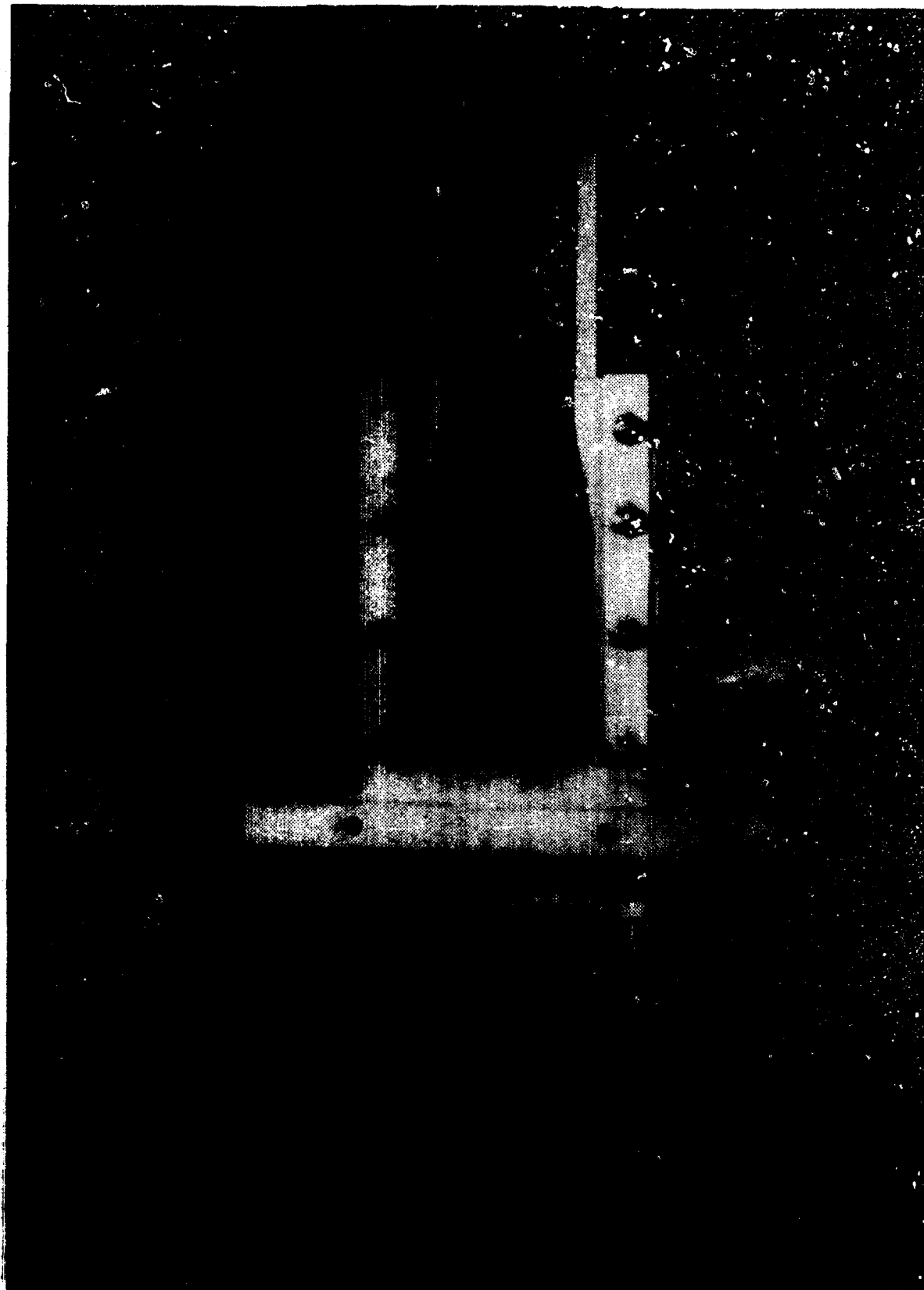
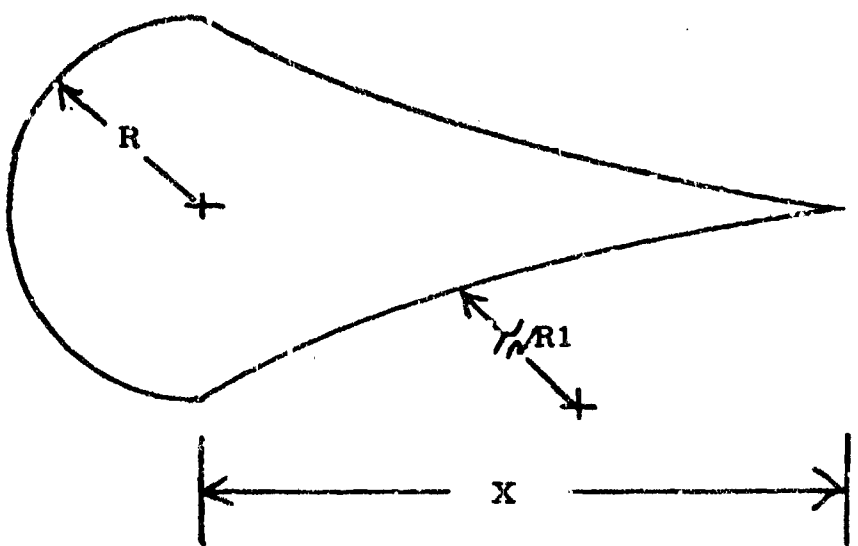
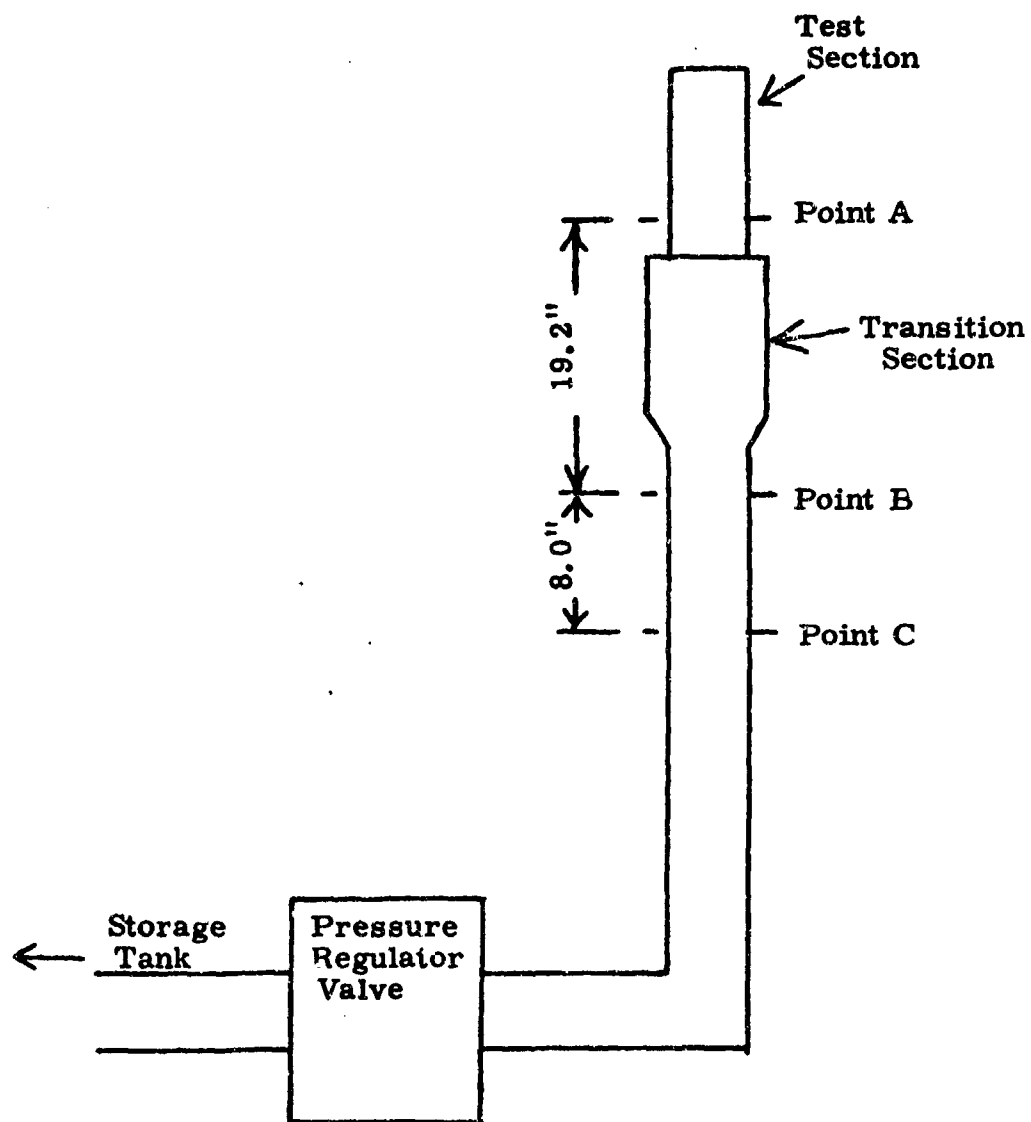


Figure 4. The Test Section.



Mach	R	X	R1
3	.250"	1.34"	3.00"
4	.605"	2.60"	6.00"

Figure 5. Nozzle Vane Detail.



**Figure 6. Experimental Set Up Showing the Location of Pressure Taps A, B, and C.**

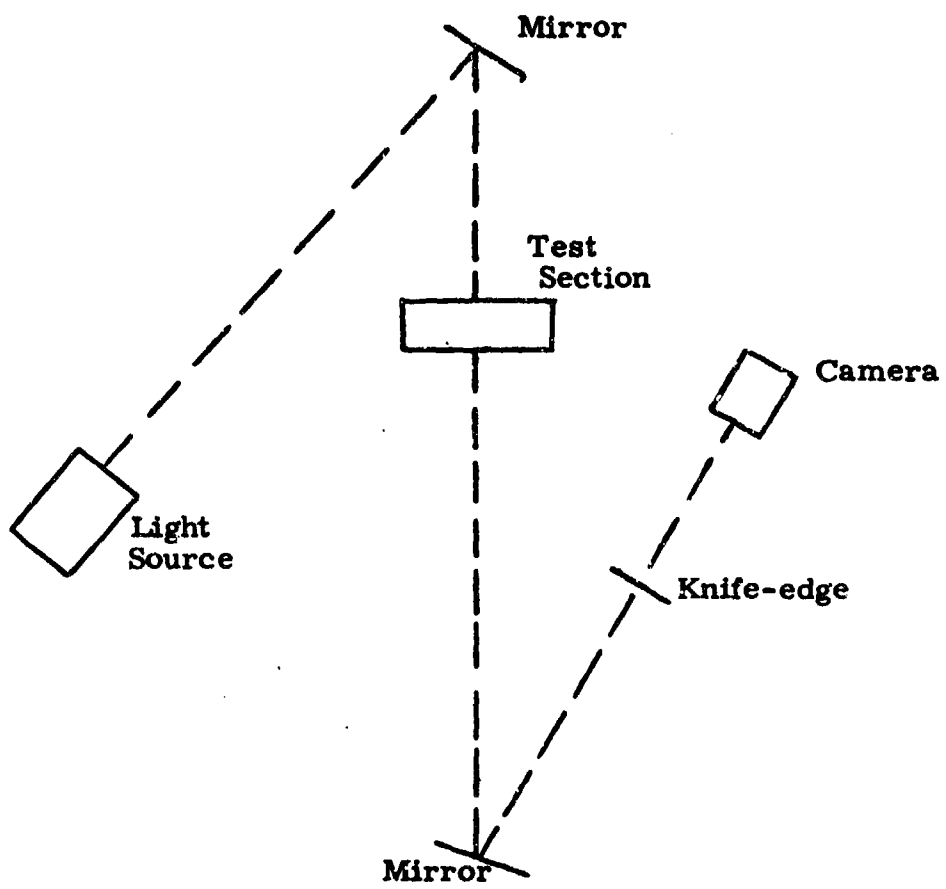
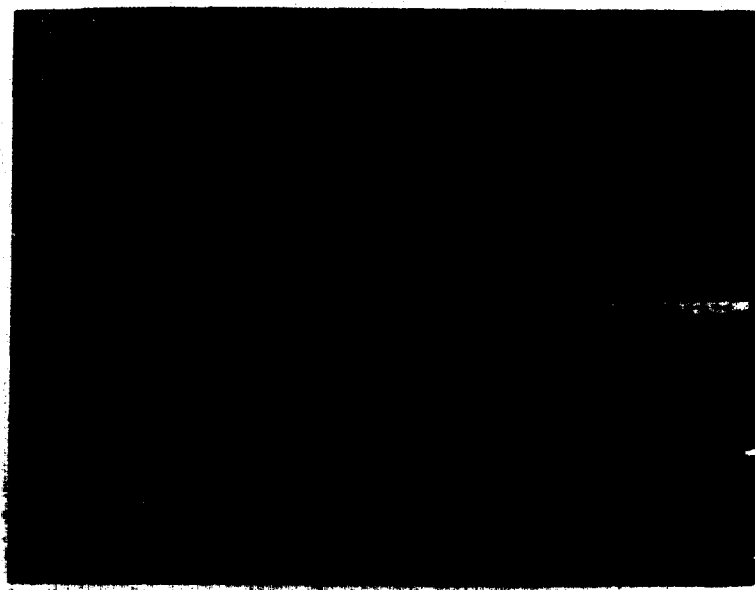


Figure 7. Diagram of the Schlieren System.



**Figure 8.** Total pressure time trace for a fast start.  
Maximum pressure 100 psig. Horizontal scale  
0.1 sec./cm.



**Figure 9.** Total pressure time trace for a fast start.  
Maximum pressure 200 psig. Horizontal scale  
0.05 sec./cm.

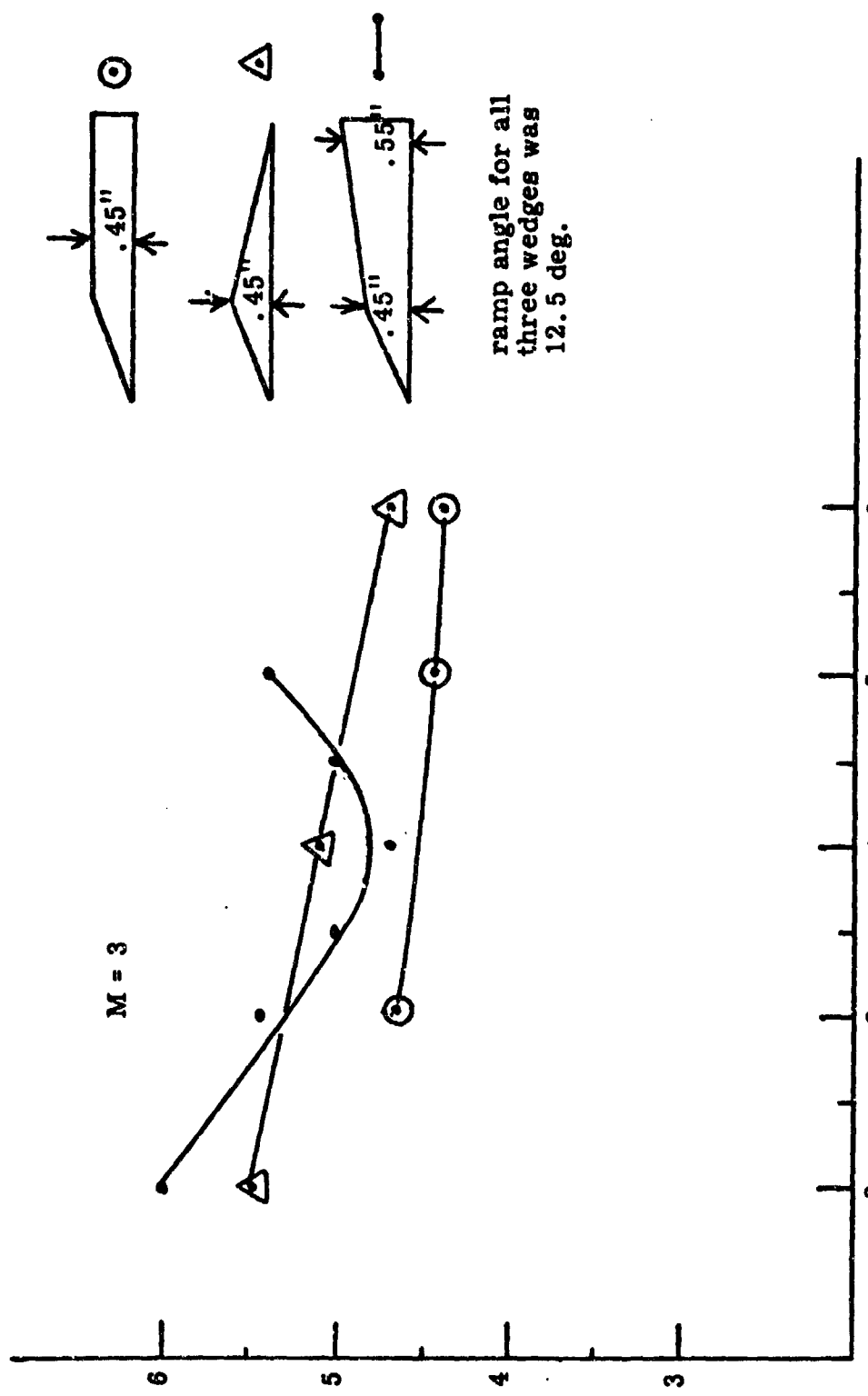
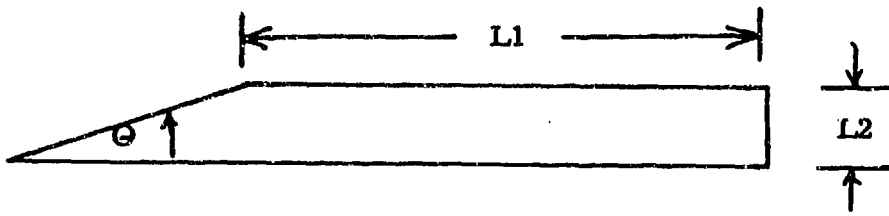


Figure 10. Graph of  $P_t/P_a$  vs. Diffuser Length



Diffuser Variables.

Legend for the graphs which follow.

$P_t$  is the total pressure.

$P_a$  is the atmospheric pressure.

$L_1$  and  $L_2$  are in inches.

$\Theta$  is in degrees.

$\odot$  indicates start not achieved at that point.

Numbered data points

No.	$L_2$	Contraction Ratio
1	.35"	.825
2	.40"	.800
3	.45"	.775
4	.50"	.75
5	.55	.725
6	.60	.70
7	.65	.675

Figure 11. Legend for following graphs and diffuser variables.

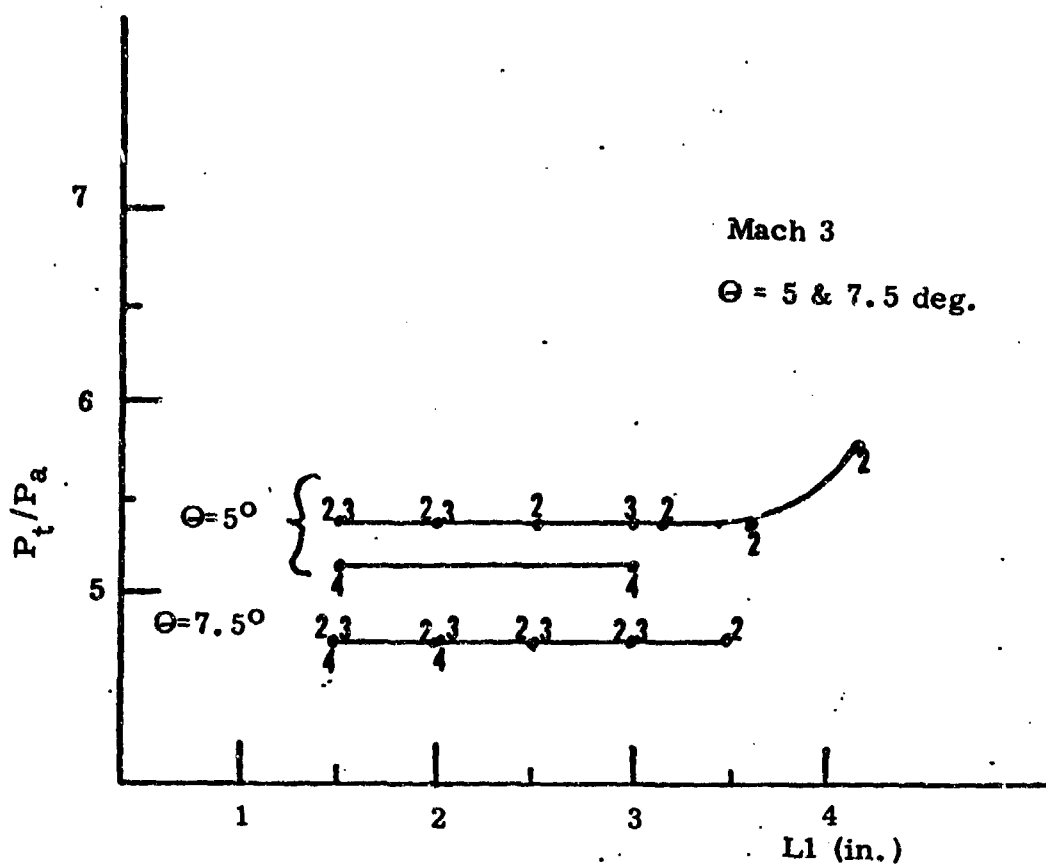


Figure 12.  $P_t/P_a$  vs.  $L1$ . Mach 3.

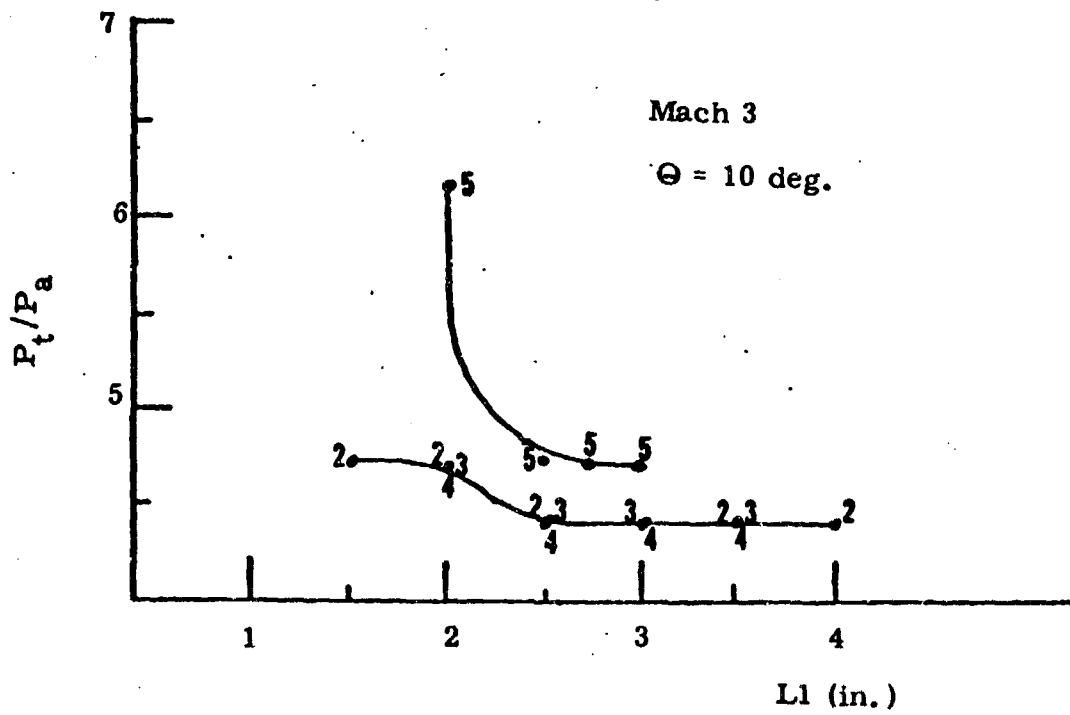


Figure 13.  $P_t/P_a$  vs.  $L1$ . Mach 3.

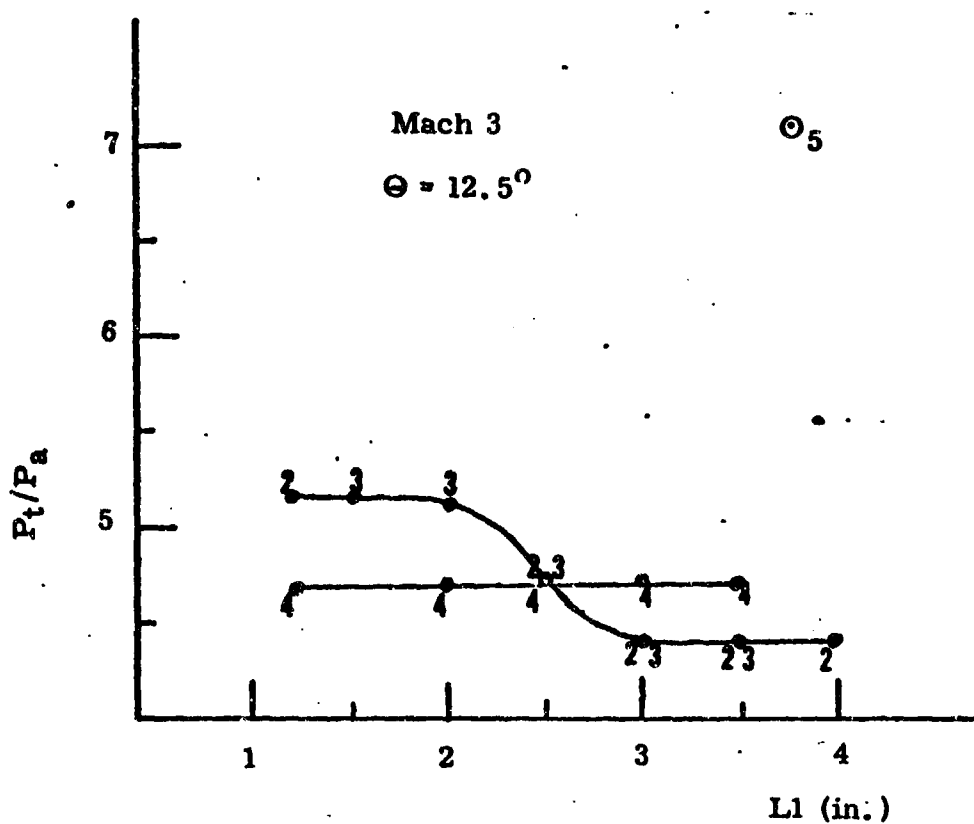


Figure 14.  $P_t/P_a$  vs.  $L_1$ . Mach 3.

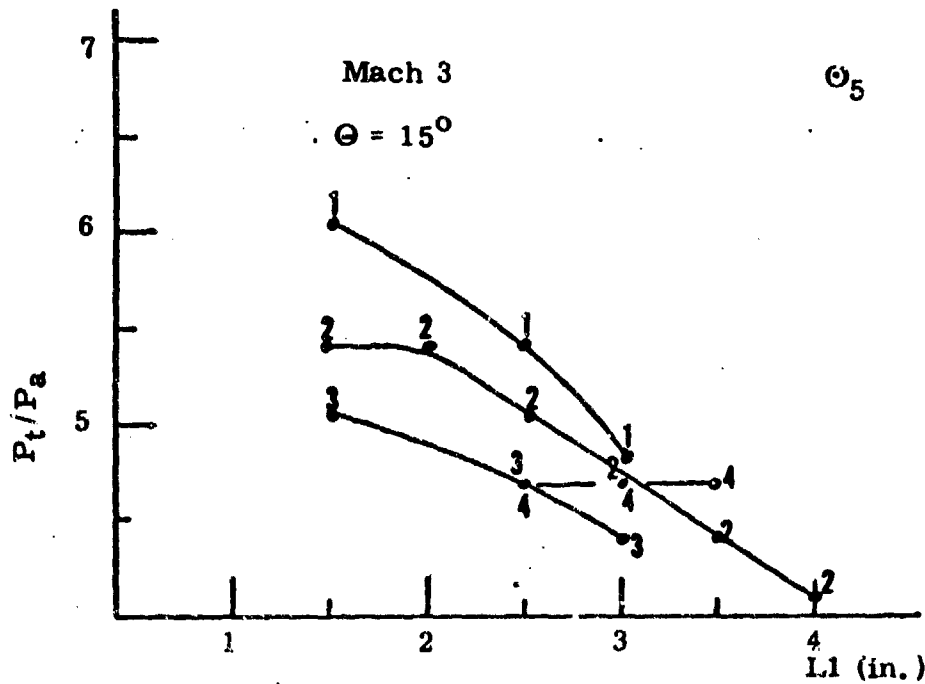


Figure 15.  $P_t/P_a$  vs. Li. Mach 3.

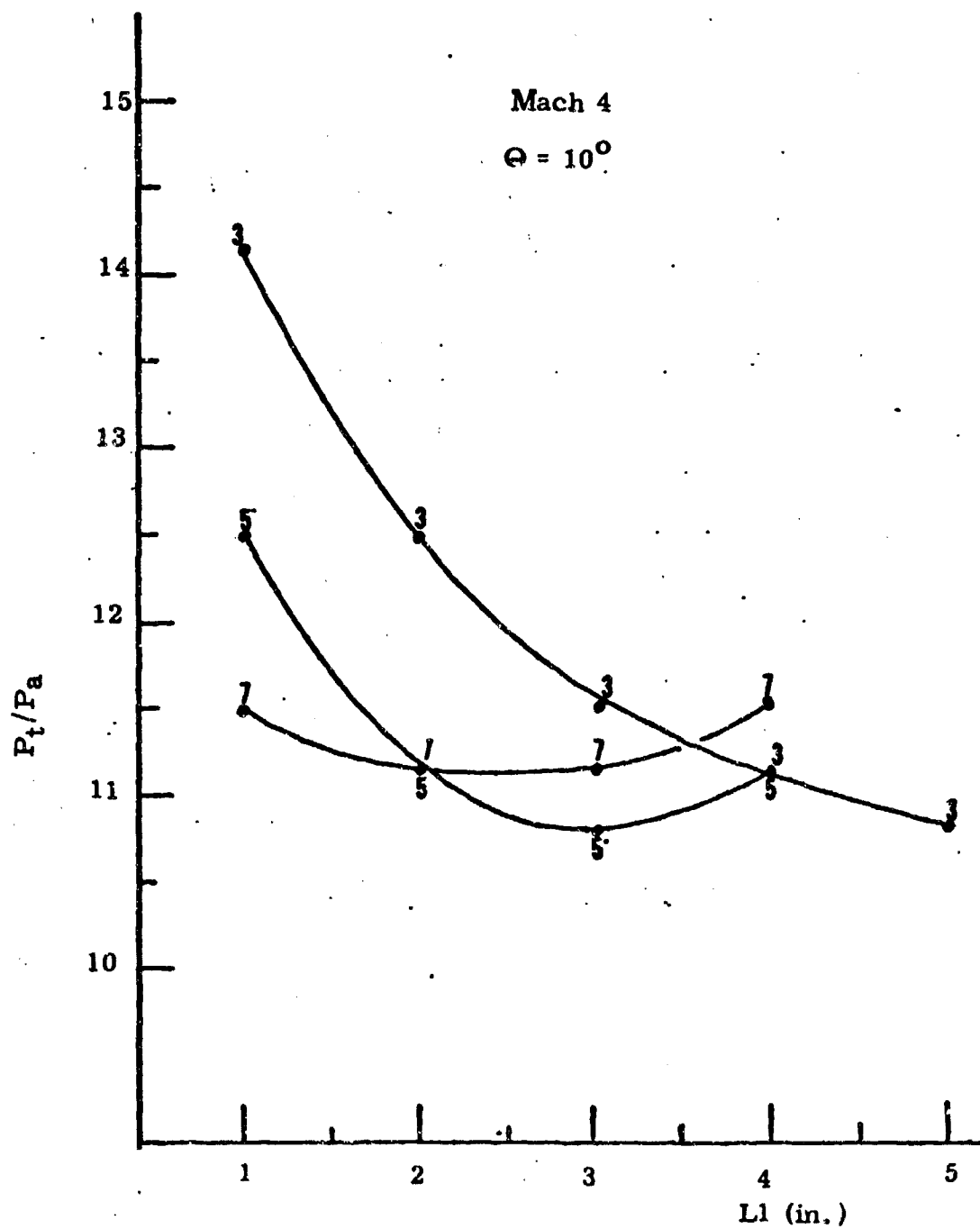


Figure 16.  $P_t/P_a$  vs.  $L1$ . Mach 4..

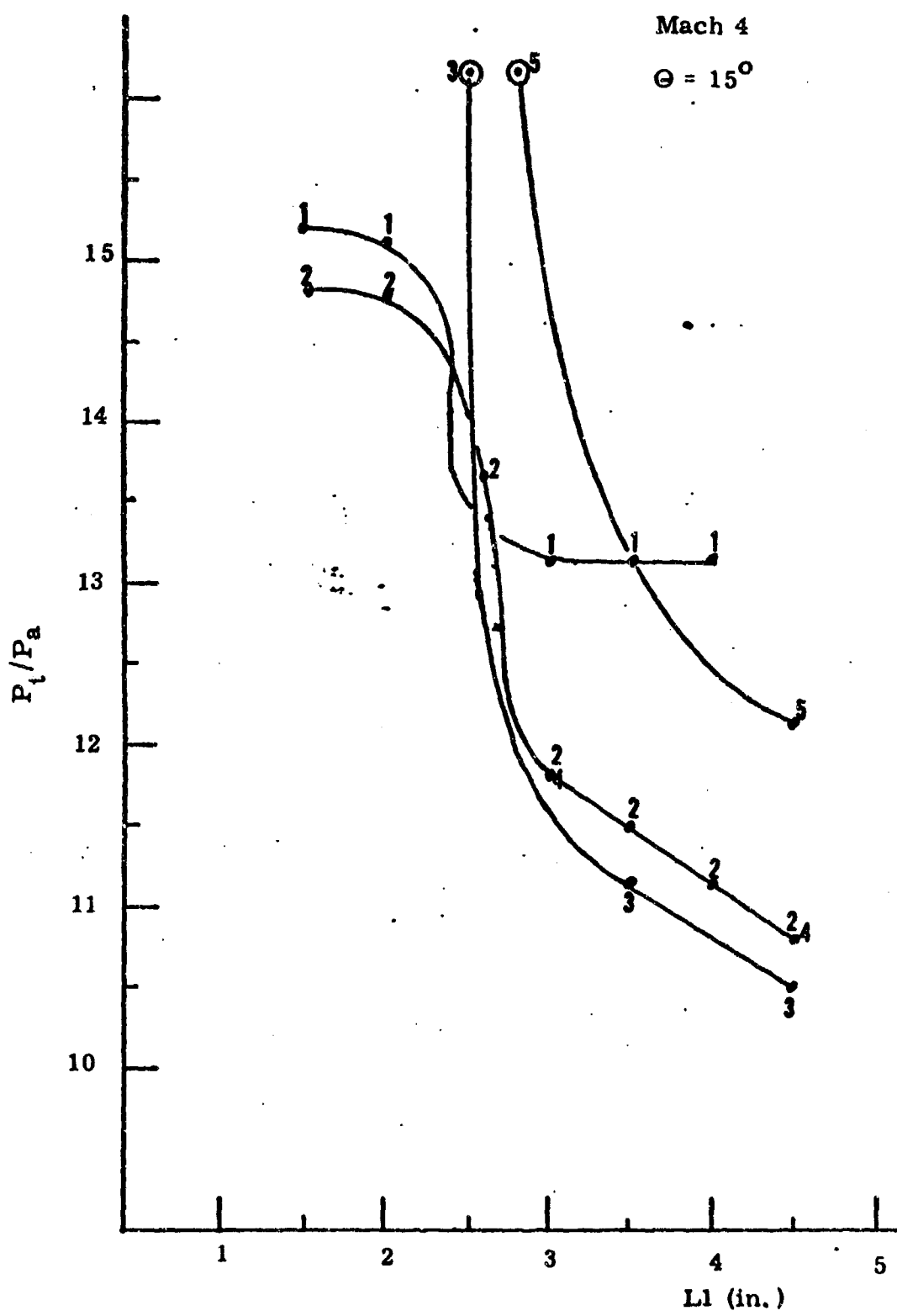


Figure 17.  $P_t/P_a$  vs.  $L1$ . Mach 4.

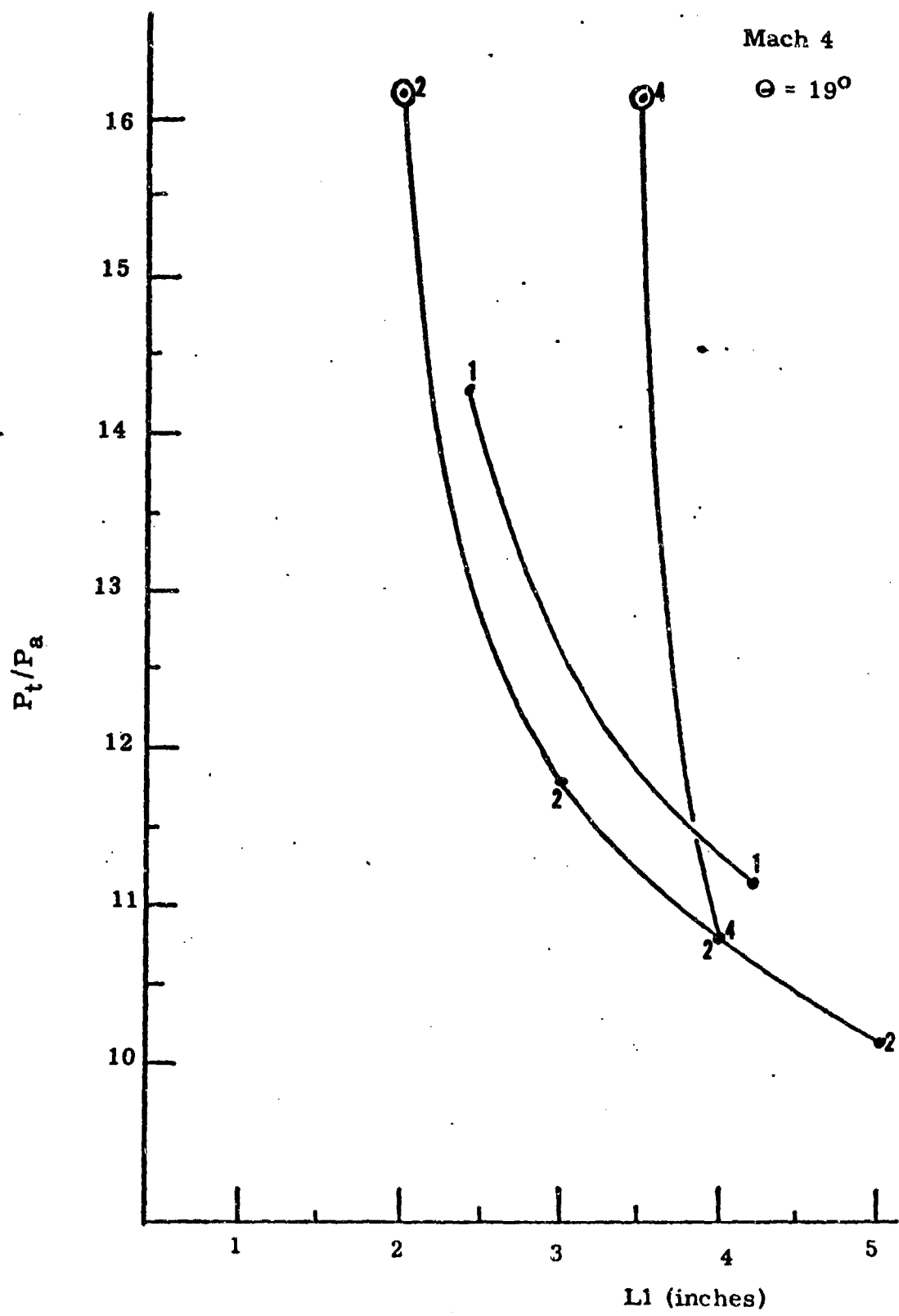


Figure 18.  $P_t/P_a$  vs. L1. Mach 4.

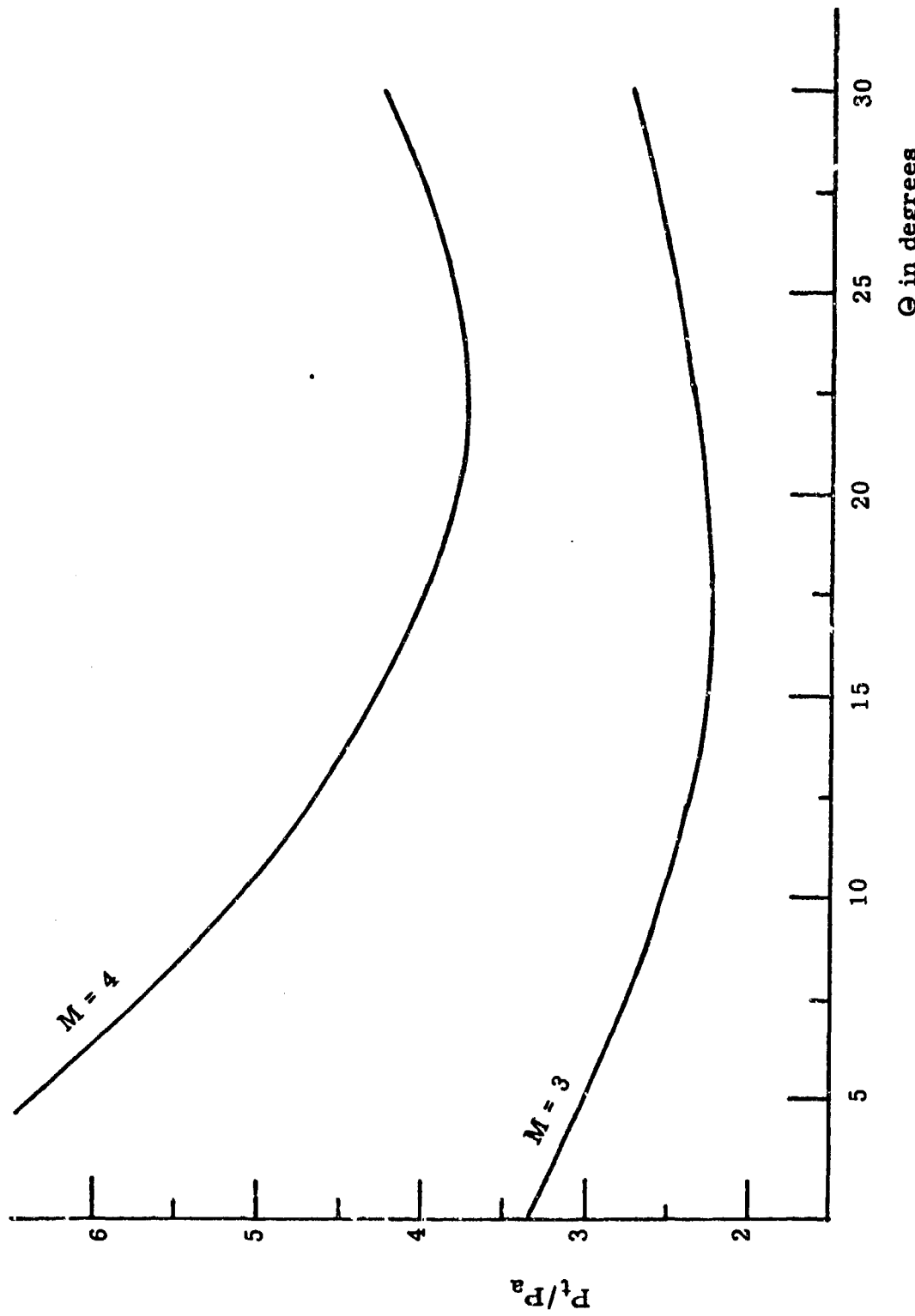


Figure 19.  $P_t/P_a$  vs.  $\Theta$ , theoretical.

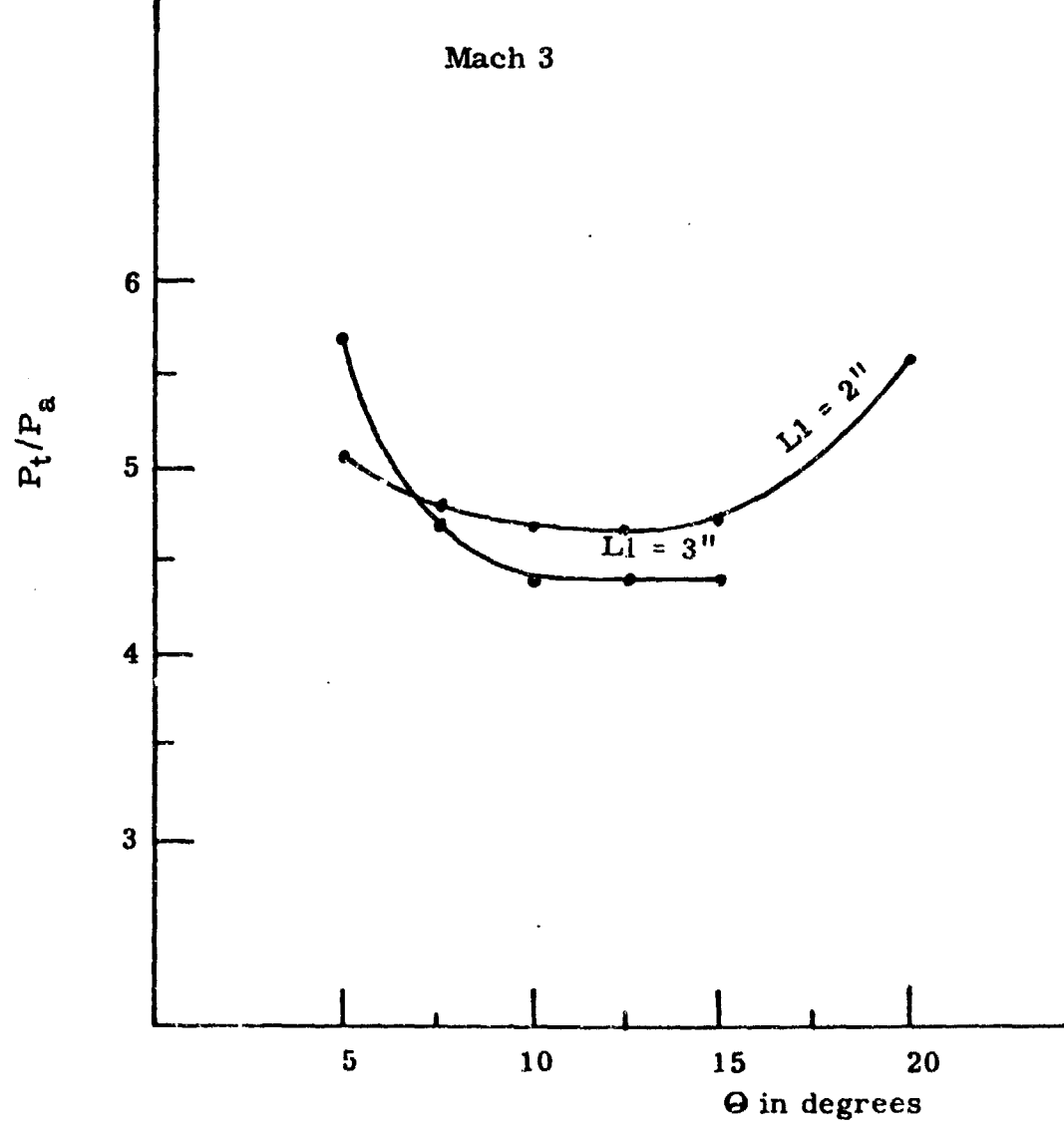


Figure 20.  $P_t/P_a$  vs.  $\Theta$ , Mach 3.

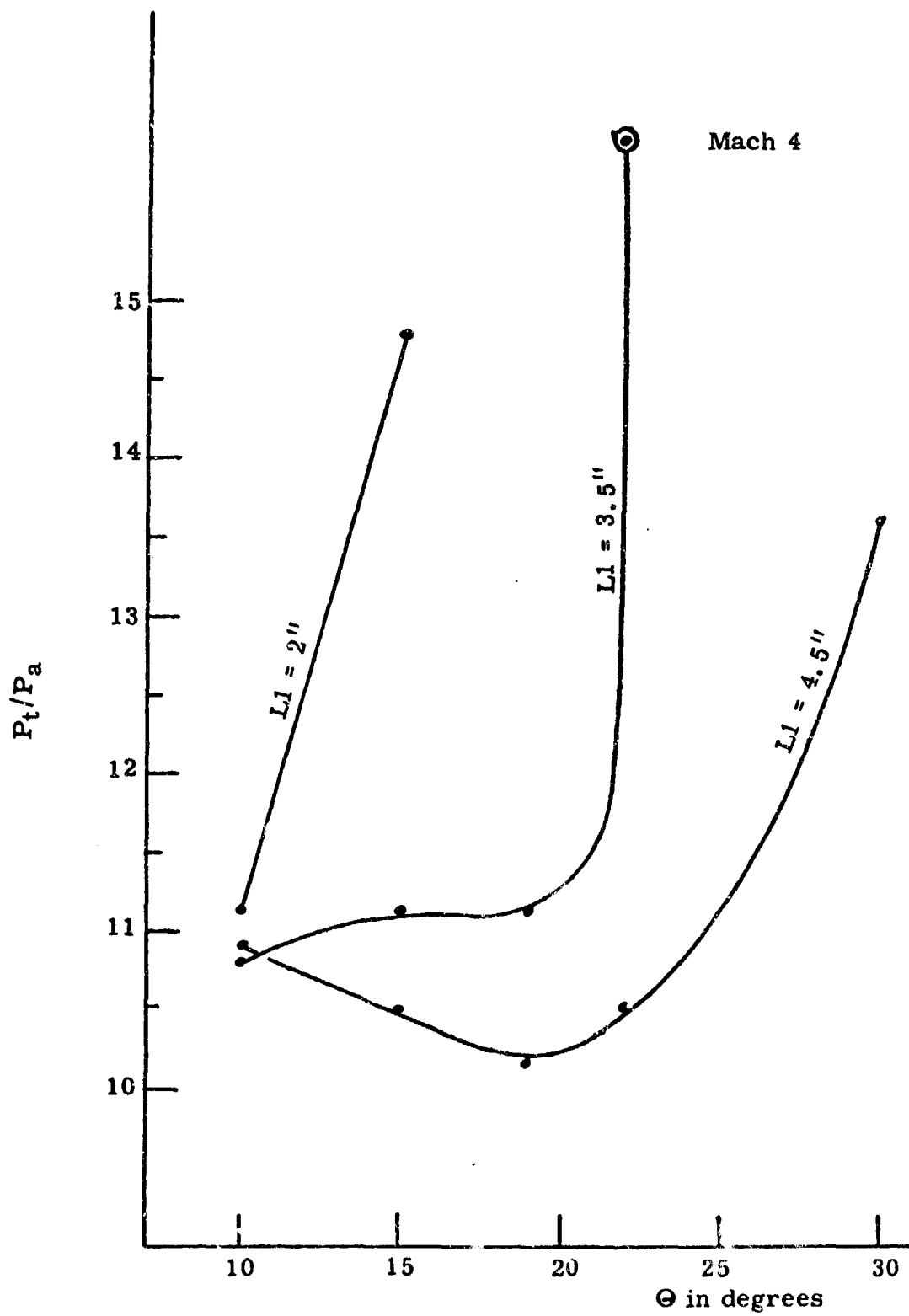


Figure 21.  $P_t/P_a$  vs.  $\Theta$ , Mach 4.

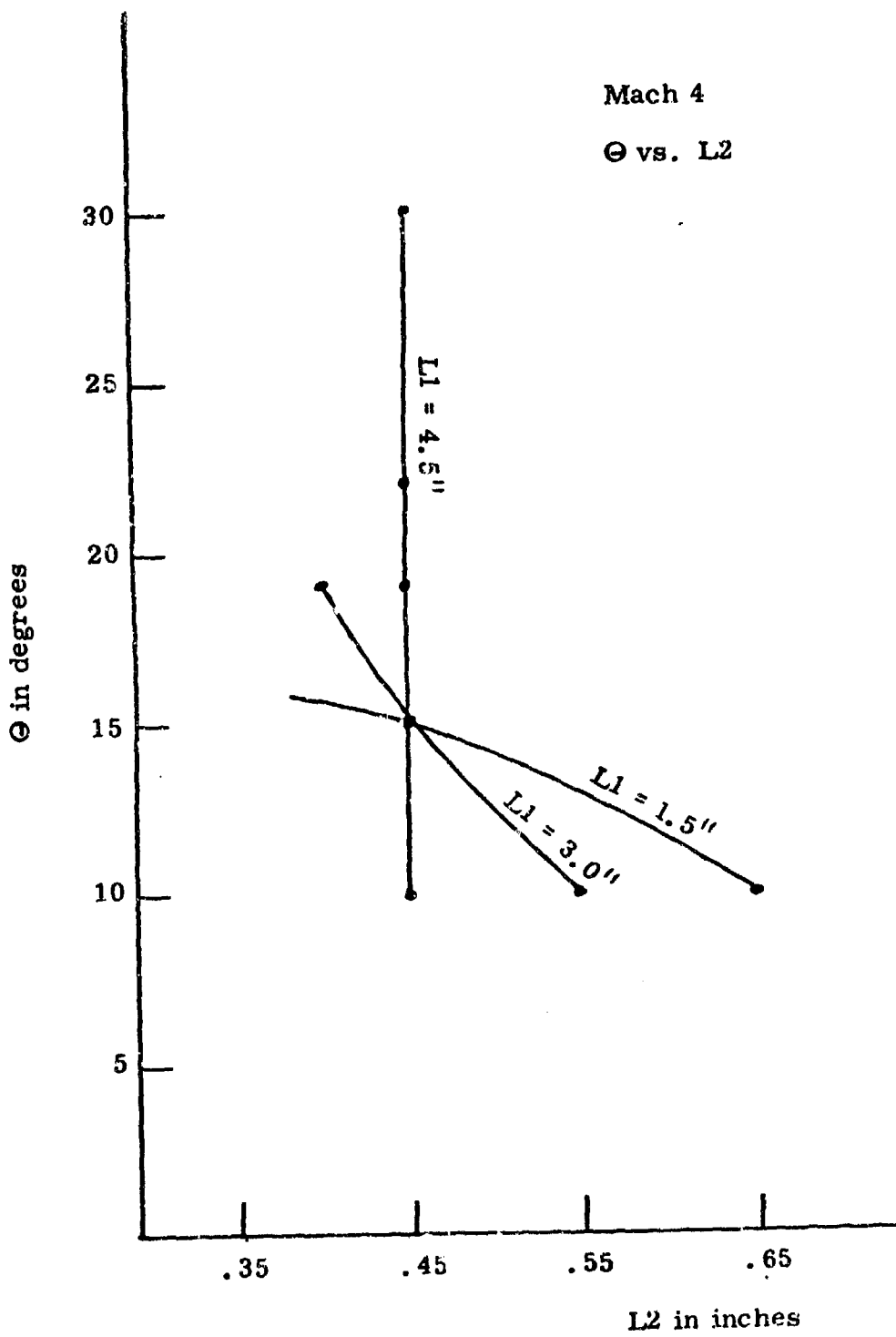


Figure 22.  $\Theta$  vs.  $L_2$  for optimum  $P_t/P_a$ .

BEST AVAILABLE COPY



Figure 23. Separated Mach 3 flow.



Figure 24. Two wedge diffusers with center plate. Mach 3.

BEST AVAILABLE COPY



Figure 25. Non-symmetric diffuser arrangement. Mach 3.

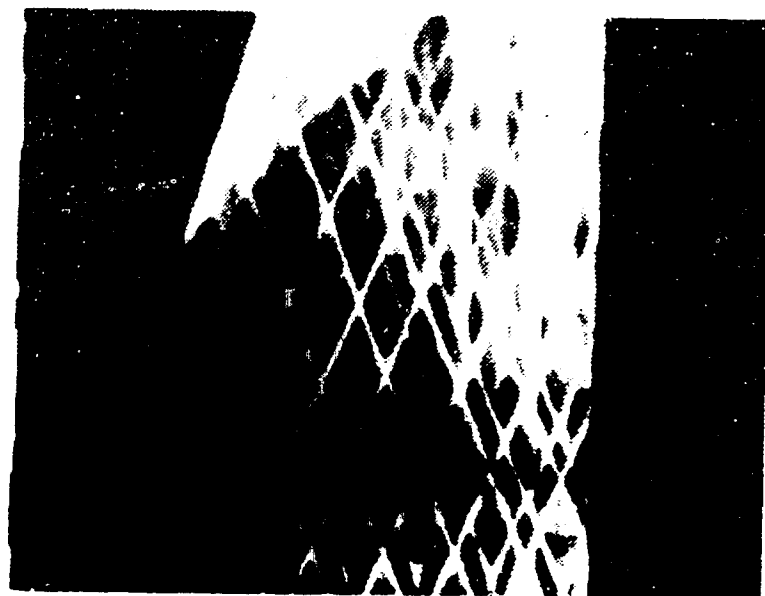


Figure 26. One-sided diffuser. Mach 3.



Figure 27. Schlieren of Mach 3 flow with no diffuser installed.

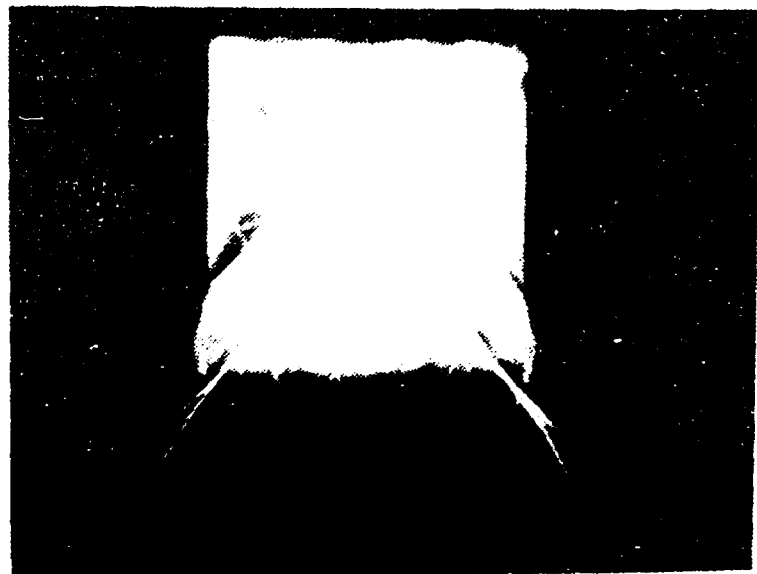


Figure 28. Fully attached diffuser flow. Mach 3.

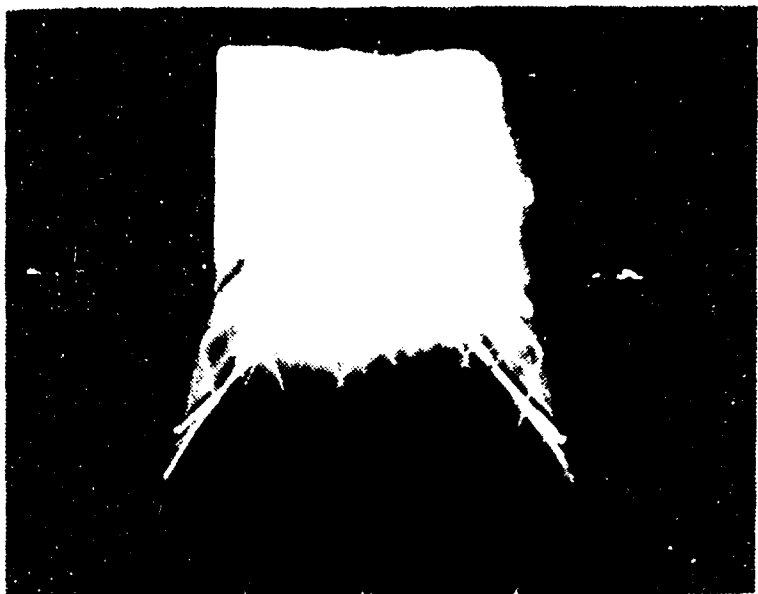


Figure 29. Flow separated from one diffuser wall. Mach 3.



Figure 30. Flow separated from both diffuser walls. Mach 3.



Figure 31. Schlieren of Mach 4 flow with a 10 degree ramp.



Figure 32. Mach 4 flow with a 15 degree ramp.

BEST AVAILABLE COPY



Figure 33. Mach 4 flow with a 19 degree ramp.

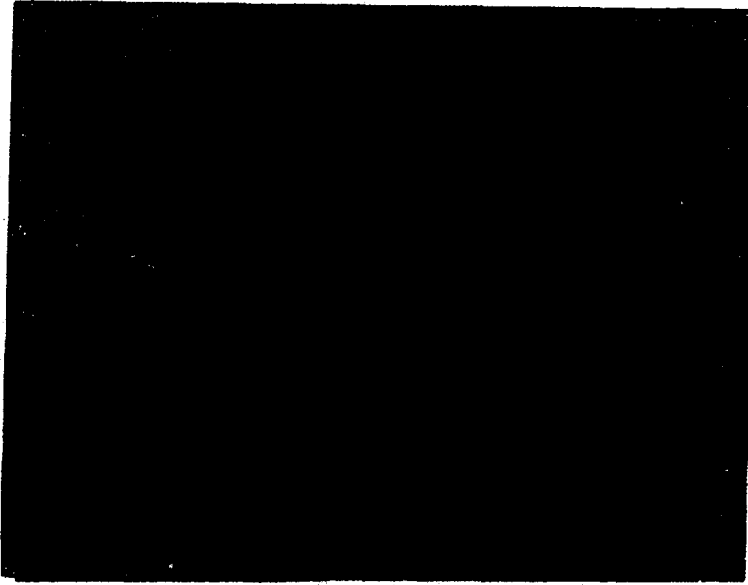


Figure 34. Pressure-time trace for Mach 3.  
Horizontal scale 0.02 sec./cm.

BEST AVAILABLE COPY

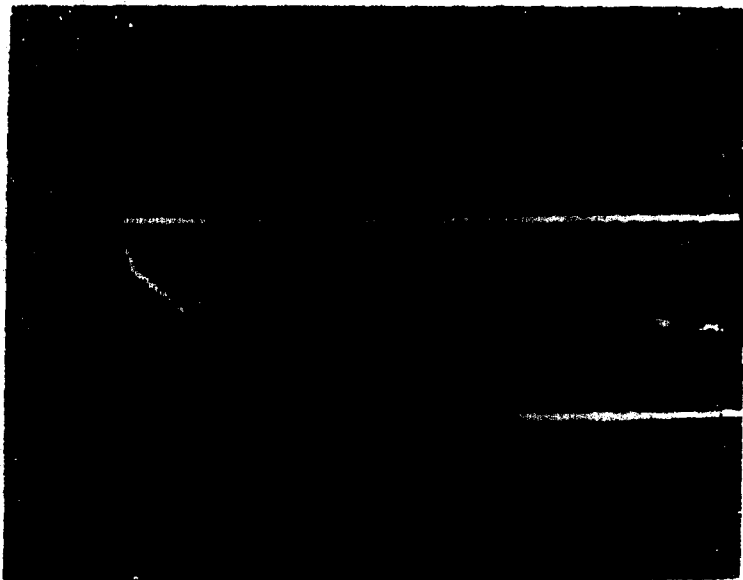


Figure 35. Cavity pressure-time trace, Mach 4. The straight line 2 squares from the top of the scale is atmospheric pressure. Horizontal scale 0.02 sec. per cm.



Figure 36. Pressure-time trace for Mach 4. Horizontal scale 0.01 sec./cm.

## LIST OF REFERENCES

1. NAVORD Report 1570, Diffuser Investigations in a Supersonic Wind Tunnel, by J. L. Diggins, 1951.
2. Neumann, W. E. and Lustwerk, F., "High Efficiency Supersonic Diffusers," J. Aero. Sci., 18, p. 369-374, 1951.
3. AIAA paper No. 69-447, A two Dimensional, Mixed Compression Inlet System Designed to Self Restart at a Mach Number of 3.5, by W. E. Anderson and N. D. Wong.
4. Major M. F. Sarabia, USAF, report presented to Laser Diffuser Workshop held at Kirkland Air Force Base, N. M., 4 December 1973.
5. AFWL Technical Report No. 71-83, Starting and Pressure Recovery in Fixed Throat Supersonic Diffusers, by T. Jones and S. Neice.
6. Purdue University TSPC-73-1, Gas Dynamics of Cavities in Series GDL: Survey and Extension, by S. N. B. Murthy.
7. Shapiro, A. H., The Dynamics and Thermodynamics of Compressible Fluid Flow, p. 1156, Ronald Press, 1954.
8. Major C. F. Dean, USAF, report presented to Laser Diffuser Workshop held at Kirkland Air Force Base, N. M., 4 December 1973.
9. NACA technical Note 3545, Investigation of the Effect of Short Fixed Diffusers on Starting Blow Down Jets in Mach Number range of 2.7 to 4.5, by J. A. Moore, 1956.
10. Shapiro, A. H., The Dynamics and Thermodynamics of Compressible Fluid Flow, p. 1148, Ronald Press, 1954.
11. Schlichting, H., Boundary Layer Theory, p. 351, McGraw Hill, 1968.
12. NASA TT-F-11665, Shock and Restart Control Systems with Bypass Doors and Pressure Transducers for Mixed Compression Inlets.
13. NACA RM E50BOZ, An Experimental Investigation of Two Internal Compression Air Inlet Designs Which Use Fluid Boundaries as a Means of Supersonic Compression, by R. Howell and P. Prescott, May, 1950.

14. Aanerud, K., Analytical Investigation of Transient Diffuser Wave Phenomena, M. S. A. E. Thesis, Naval Postgraduate School, 1974.
15. Imperial College of Mech. Eng. Report UF/TN/O/2, Procedure for Calculating the Unsteady, One Dimensional, Flow of a Compressible Fluid with Allowance for Heat Transfer and Friction, D. B. Spalding, London, 1969.
16. Reneau, L. R., Johnston, J. P., and Kline, S. J., "Performance and Design of Straight, Two-Dimensional Diffusers," p. 8.